Biomedical Signal Processing and Control 80 (2023) 104291

Contents lists available at ScienceDirect

Biomedical Signal Processing and Control

journal homepage: www.elsevier.com/locate/bspc

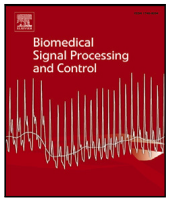

Effects of noise and filtering strategies on the extraction of pulse rate variability from photoplethysmograms

Elisa Mejía-Mejía *, Panicos A. Kyriacou

Research Centre for Biomedical Engineering, City, University of London, London, United Kingdom

ARTICLE INFO

Keywords:
Photoplethysmography
Pulse rate variability
Synthetic PPGs
Simulation
Noise
Filtering

ABSTRACT

Pulse rate variability (PRV) describes the changes in pulse rate through time, when measured using pulsatile signals such as photoplethysmograms (PPG). PRV has been used as a surrogate of heart rate variability (HRV), but their relationship is not straightforward, both due to physiological differences and to effects of technical aspects on the extraction of PRV information from pulsatile signals such as the PPG. One of the factors that may affect PRV analysis is the presence of noise and the filtering strategy used to pre-process the PPG signal. In this study, the aim was to evaluate the best performing filtering strategy for the extraction of PRV information reliably from noise-contaminated synthetic PPG signals. Time domain, frequency domain and Poincaré plot indices were extracted from PRV trends obtained from the filtered PPG signals and compared against indices measured from a gold-standard simulated PRV function. It was found that PRV information can be reliably extracted from PPG signals filtered using lower low cutoff frequencies and elliptic IIR or equiripple or Parks–McClellan FIR filters, however the filtering parameters depend on the type of noise present in the signal. Moreover, special care should be taken to assess the pNN50 index from contaminated PPG signals, regardless of the type of noise. Future studies should aim to validate these results from real PPG data.

1. Introduction

Pulse rate variability (PRV) refers to the changes in pulse rate through time [1]. It is extracted from pulsatile signals such as photoplethysmograms (PPGs), and has been proposed as an alternative to the measurement of heart rate variability (HRV), which relies on the acquisition and processing of electrocardiographic signals [2]. Due to the widespread availability of PPG sensors, especially in wearable devices [3], PRV extracted from PPGs has been gaining attention in the last decades, and researchers have used it for several applications, including the monitoring and prediction of mental and cardiovascular diseases [1].

Nonetheless, the relationship between HRV and PRV is not entirely understood, and there is evidence of a different behaviour on these two variables under different circumstances. It has been demonstrated that physiological aspects, such as changes in blood pressure, pulse transit time and respiration, may affect PRV in a different way than HRV [4–8]. Also, technical aspects have been proposed as important causes for the differences between HRV and PRV. Some of the factors that has been considered as possible contributors to these differences are the sampling rate used for acquire the PPG, the fiducial points used for the detection of the inter-beat intervals (IBIs) from the PPG, and the pre-processing strategies used for extracting PRV from PPG signals [1,9].

The pre-processing alternatives to extract PRV information from PPG may include processes such as scaling, outlier removal, detrending, resampling and filtering. Particularly the latter one may have an important role in the reliability of PRV information, especially when noise-contaminated signals are considered, which makes it harder to extract IBIs with confidence. The aim of this study was to investigate the performance of different filtering techniques when applied to PPG signals corrupted with different types of noise. Also, the study investigated how various filters affected PRV indices, with an ultimate goal to determine the best performing filter for PRV analysis. Therefore, PPG signals were simulated with 15 different types of noise and PRV was extracted from the filtered signals. The extracted PRV indices were compared to gold-standard PRV information and the best performing filtering strategy for each kind of noise-contaminated PPG signals was determined.

2. Materials and methods

The simulation and processing of PPG signals and PRV was performed in MATLAB (version 2020b), while statistical analyses were

* Corresponding author.
E-mail address: elisa.mejia-mejia@city.ac.uk (E. Mejía-Mejía).

https://doi.org/10.1016/j.bspc.2022.104291
Received 22 July 2022; Received in revised form 13 September 2022; Accepted 8 October 2022
Available online 21 October 2022

Table 1
Ranges for the Pulse Rate Variability (PRV) parameters and the generation of PRV gold standard values.

Parameter	Range	Units
Low frequency peak location (LF)	0.04–0.15	Hz
High frequency peak location (HF)	0.15–0.40	Hz
Average pulse rate (PR)	40–200	Beats per minute (bpm)
Standard deviation of pulse rate (SD)	0.05–0.08	s

Table 2
Parameters used for the simulation of noise corrupted photoplethysmographic (PPG) signals. RES: Respiratory noise; BW: Baseline wandering; EM: Electromagnetic noise; MA: Movement artifact. A_n: Proportion of the noise amplitude with respect to the PPG signal amplitude; f: Fundamental frequency of the noise. x: Indicates the inclusion of the specific type of noise in the resulting signal.

Combination	Types of noise				Parameters	
	RES	BW	EM	MA	A_n	f (Hz)
C1	x	–	–	–	0.1	0.15
C2	–	x	–	–	0.5	[0.08, 0.18]
C3	–	–	x	–	0.1	60
C4	–	–	–	x	0.07	[1.02, 7.31, 5.06]
C5	x	x	–	–	RES: 0.1	RES: 0.15
					BW: 0.5	BW: [0.08, 0.18]
C6	x	–	x	–	RES: 0.1	RES: 0.15
					EM: 0.1	EM: 60
C7	x	–	–	x	RES: 0.1	RES: 0.15
					MA: 0.07	MA: [1.02, 7.31, 5.06]
C8	–	x	x	–	BW: 0.5	BW: [0.08, 0.18]
					EM: 0.1	EM: 60
C9	–	x	–	x	BW: 0.5	BW: [0.08, 0.18]
					MA: 0.07	MA: [1.02, 7.31, 5.06]
C10	–	–	x	x	EM: 0.1	EM: 60
					MA: 0.07	MA: [1.02, 7.31, 5.06]
C11	x	x	x	–	RES: 0.1	RES: 0.15
					BW: 0.5	BW: [0.08, 0.18]
					EM: 0.1	EM: 60
C12	x	x	–	x	RES: 0.1	RES: 0.15
					BW: 0.5	BW: [0.08, 0.18]
					MA: 0.07	MA: [1.02, 7.31, 5.06]
C13	x	–	x	x	RES: 0.1	RES: 0.15
					EM: 0.1	EM: 60
					MA: 0.07	MA: [1.02, 7.31, 5.06]
C14	–	x	x	x	BW: 0.5	BW: [0.08, 0.18]
					EM: 0.1	EM: 60
					MA: 0.07	MA: [1.02, 7.31, 5.06]
C15	x	x	x	x	RES: 0.1	RES: 0.15
					BW: 0.5	BW: [0.08, 0.18]
					EM: 0.1	EM: 60
					MA: 0.07	MA: [1.02, 7.31, 5.06]

done in RStudio (version 1.4.1717). Fig. 1 summarises the methodology proposed in this study.

2.1. Signal simulation

PPG signals were simulated using a modified version of the model proposed by Tang et al. [10,11]. In their model, a single cardiac cycle was simulated using the sum of two Gaussian functions with parameters set to obtain excellent and acceptable quality PPG signals. These parameters that describe the Gaussian functions, i.e., a_i, b_i and μ_i, were determined according to the behaviour of annotated PPG signals obtained from the MIMIC III database [12–14]. In the modified version of this model, proposed in this study, the quality of the PPG waveform can be set by modifying the ratio r of the a parameters from the two Gaussian functions, which alters the amplitude of the Gaussian functions and, therefore, determines the presence or absence of a dicrotic notch, and its amplitude. The b and μ parameters were selected according to what has been suggested in the original model for the excellent quality PPG. The resulting model for the PPG cycle is shown in (1), where θ corresponds to the four quadrant inverse tangent of the cosine and sine functions of the duration of the cycle.

$$z = a(e^{-\frac{(\theta-\mu_1)^2}{2b_1^2}}) + \frac{1}{r}a(e^{-\frac{(\theta-\mu_2)^2}{2b_2^2}}) \quad (1)$$

The duration of each of the cardiac cycles was modified in order to include PRV information on the PPG signal. This was done by simulating PRV information as a sum of sinusoidal waves with randomly generated parameters (Table 1) that fall inside plausible physiological ranges for PRV.

The resulting function for the randomly generated PRV information is shown in (2). As can be seen, a total of four sinusoidal waves were summed, each of them with different fundamental frequencies, two for each of the main frequency bands as found in PRV analysis. This was done to increase the variability of the frequency spectrum and to alter the area of each of the frequency bands. This function was used as gold-standard for the comparison of PRV extracted from the PPG signals.

$$PRV = PR + SD\sum_{i=1}^{2}(\sin(2\pi LF(i)t) + \sin(2\pi HF(i)t)) \quad (2)$$

Simulated cardiac cycles were appended and the resulting signal was detrended and low pass filtered using a second-order Butterworth filter with cutoff frequency of 15 Hz. In this study, two types of PPG signals were simulated, according to the ratio r used to simulate the amplitude of the Gaussian functions. Excellent quality PPG signals were simulated with ratios of $r = 2$, while acceptable quality PPG signals were considered as those with $r = 4$. The base cardiac cycles for these two values of r are illustrated in Fig. 2. The main difference between these signals can be observed in the notoriety of the dicrotic notch, i.e., its amplitude when compared to the amplitude of the systolic peak. Fig. 3 depicts excellent and acceptable PPG signals simulated using the model with the specified r values, and with randomly generated PRV information.

The proposed simulation framework allows also for the inclusion of four different types of noise to the PPG signal or any of their combinations. These noises were respiratory noise, baseline wandering, electromagnetic noise and movement artifact. The mathematical model for the respiratory noise follows an amplitude modulation method, and is shown in (3), where $x(t)$ and $y(t)$ represent the clean and noisy PPG signals. There are two parameters that can be modified for this type of noise, the proportion of noise amplitude with respect to the amplitude of the PPG signal, A_n, and the fundamental frequency for the respiratory noise, f [Hz].

$$y(t) = \max(x(t))[1 + A_n(\sin(2\pi f t))]x(t) \quad (3)$$

The mathematical model for baseline wandering noise is similar, as shown in (4), but allows for the selection of N frequency components for the noise. In this case, the parameters are also the proportion of amplitudes, A_n, and the fundamental frequencies of each of the sinusoidal waves to add as noise.

$$y(t) = \max(x(t))[1 + A_n\sum_{i=1}^{N}(\sin(2\pi f(i)t))]x(t) \quad (4)$$

The electromagnetic noise is added as shown in (5), and the same two parameters, A_n and f, can be modified accordingly.

$$y(t) = x(t) + A_n[\max(x(t))]\sin(2\pi f t) \quad (5)$$

Finally, the model for the movement artifact is shown in (6). It consists in the summation of N sinusoidal waves, each of them with a fundamental frequency f within 1 and 10 Hz. The proportion of amplitudes A_n allows for the modification of the signal-to-noise ratio, as with the previously described types of noise.

$$y(t) = x(t) + A_n[\max(x(t))]\sum_{i=1}^{N}\sin(2\pi f(i)t) \quad (6)$$

Fig. 4 illustrates the resulting PPG signals when simulated without noise and with each of the described noise types.

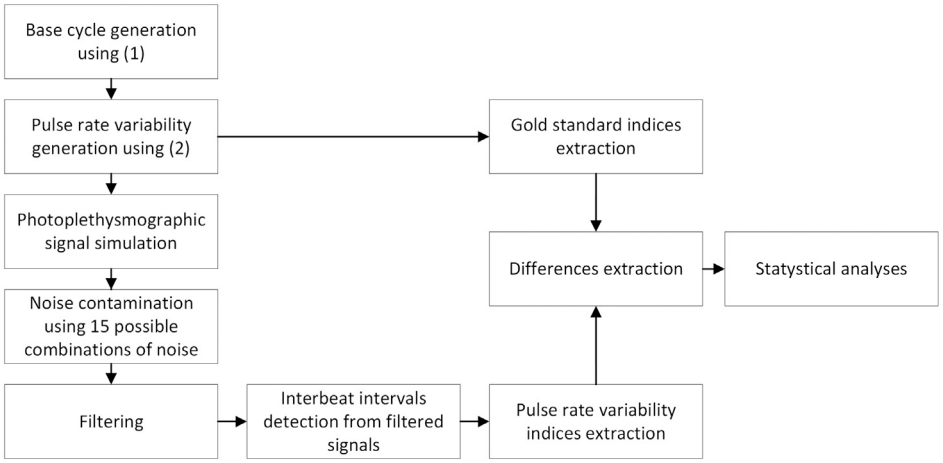

Fig. 1. Flow diagram of the methodology employed in this study.

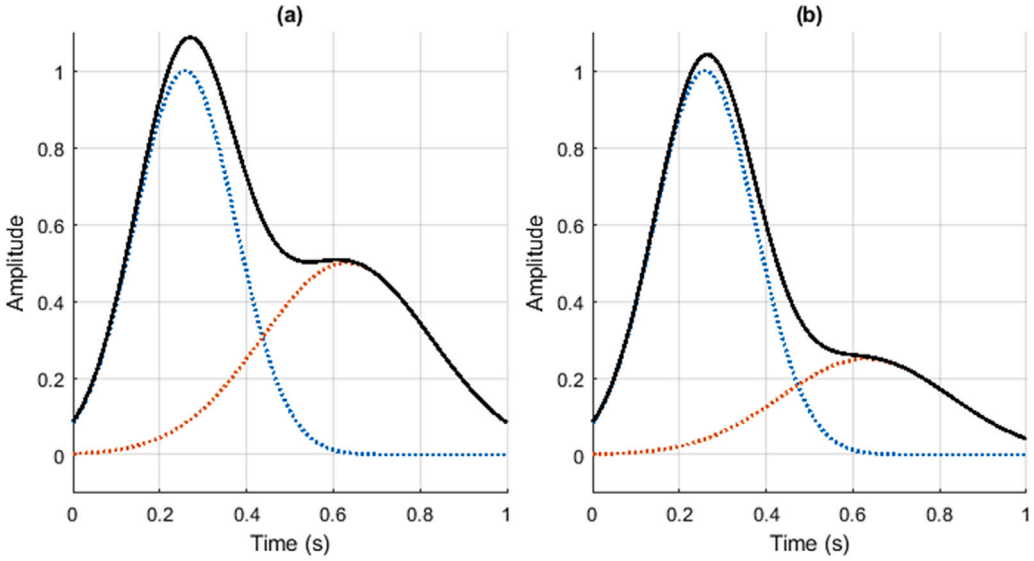

Fig. 2. Photoplethysmographic cardiac cycles generated using the proposed model, using ratios of value (a) $r = 2$ (excellent quality), and (b) $r = 4$ (acceptable quality). The blue and orange dotted lines illustrate the two Gaussian functions generated, while the black continuous line shows the result of summing these two Gaussian functions, i.e., z.

For this study, PPG signals were simulated with 15 different types of noise achieved by applying all possible combinations of the 4 types of noise that can be simulated with the proposed framework. Table 2 summarises these combinations and the parameters used for the generation of noise. A total of 117 excellent and 117 acceptable quality PPG signals for each of the noise combinations were simulated. These signals were 5 min long and had a 256 Hz sampling rate, which has been shown to be a good sampling rate for PRV analysis from PPG signals [9,15].

2.2. Filtering strategies

Different types of filters were designed in order to evaluate which filtering strategy produces more reliable PRV indices extracted from the simulated noise-corrupted PPG signals. Both finite (FIR) and infinite impulse response (IIR) filters were considered, with different orders and low and high cutoff frequencies.

For FIR filters, 5 design methods were considered: Equiripple filter (FIREQR), Hamming window (FIRWIN), constrained least squares (FIRCLS), least squares (FIRLS) and Parks–McClellan (FIRPM). For FIREQR and FIRPM, the optimal order was determined using MATLAB built-in functions, whereas for the remaining FIR filters, the sampling rate $f_s = 256$ Hz was used as the order of the filter. In all cases, a 3 dB passband ripple and a 40 dB stopband attenuation were considered. Similarly, two design methods were considered for IIR filters, i.e., Butterworth (IIRBUT) and Elliptic (IIRELL) filters. For these filters, the order was also optimised using MATLAB built-in functions, and 3 dB and 40 dB were considered as passband ripple and stopband attenuation, respectively. A total of 210 filters were designed by combining these parameters and the investigated values of low and high cutoff frequencies. Low cutoff frequencies considered were $f_{c,low} \in [0.0, 0.1, 0.2, 0.5, 1.0, 2.0]$ Hz, while high cutoff frequencies were $f_{c,high} \in [8, 10, 12, 15, 20]$ Hz.

2.3. Pulse rate variability assessment

The designed filters were applied to the noise-corrupted simulated PPG signals, and IBIs were detected from the filtered signals using the algorithm described in [16]. This algorithm is based on the generation of blocks of interests using two moving averages, which are designed according to the expected duration of cardiac cycles and the a point in the second derivative of the PPG signal. The location of the systolic peak from the PPG signal was determined as the location of the maximum point in each block of interest. This algorithm has been found to have a good performance for PRV analysis [9]. IBIs were then obtained

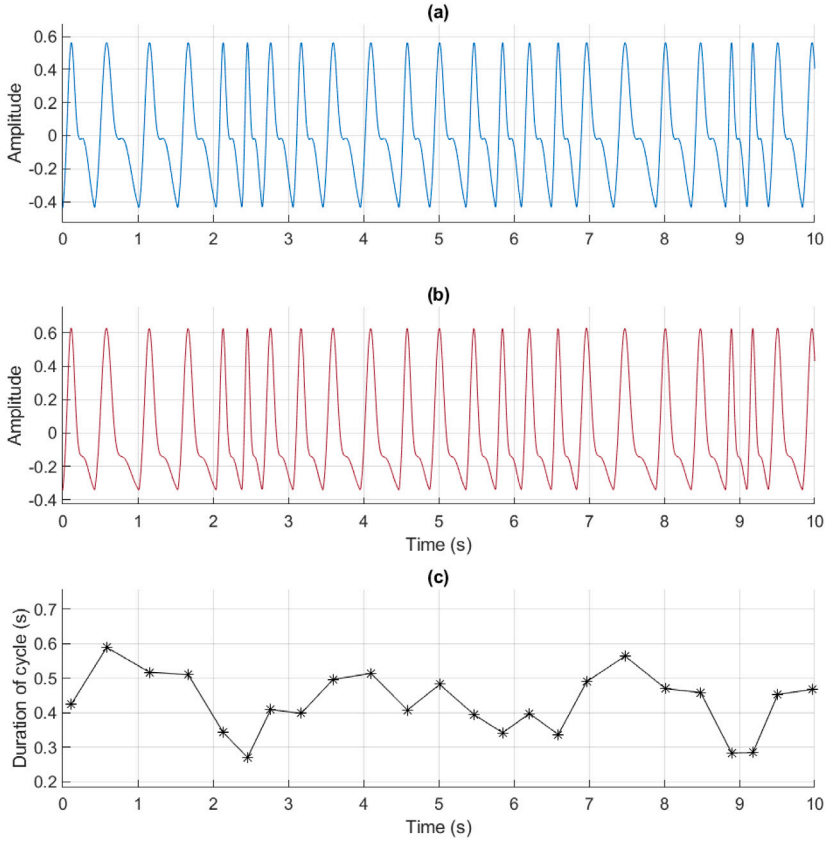

Fig. 3. Example of photoplethysmographic (PPG) signals simulated using the proposed model and randomly generated pulse rate variability (PRV) information. (a) PPG signal with excellent quality ($r = 2$). (b) PPG signal with acceptable quality ($r = 4$). (c) PRV information used for the generation of these signals.

as the time difference between consecutive a points detected from each of the identified cardiac cycles. IBIs longer than 1.25 times the median duration of all the IBIs were corrected by looking for additional cardiac cycles in each of these longer windows. IBIs shorter than 0.75 times the median duration of IBIs were also detected and discarded.

PRV indices were then extracted from the time series created using the IBIs, as well as from the gold-standard PRV functions. The average duration of cardiac cycles (AVNN), the standard deviation of this duration (SDNN), the root-mean square value of the successive differences between consecutive IBIs (RMMSD) and the proportion of successive differences larger than 50 ms (pNN50) were used to describe the behaviour of PRV trends in the time domain. Additionally, 1-lag Poincaré plot indices were used to assess the non-linear behaviour of PRV. Hence, the ellipse-fitting technique was used to extract information from the Poincaré plot, and the area of the ellipse (S), the major and minor axes of the ellipse (SD2 and SD1) and the ratio between the axes (SD1/SD2) were measured.

Finally, PRV trends were interpolated using a cubic-spline interpolation and an interpolation frequency of 4 Hz. Spectral analysis was then performed using the fast Fourier transform (FFT) with 512 points. From the obtained spectra, the absolute power of the very-low ($0.0033 \leq f < 0.04$ Hz, VLF), low ($0.04 \leq f < 0.15$ Hz, LF) and high ($0.15 \leq f \leq 0.4$ Hz, HF) frequency bands, as well as the total power (TP) between 0.0033 and 0.4 Hz were extracted. Relative power from the LF and HF bands (nLF and nHF, respectively), and the ratio between LF and HF (LF/HF) were also measured. Finally, the behaviour of these frequency bands was characterised by measuring the $x-$ and $y-$coordinated of the centroid of the band (cLF_x, cLF_y, cHF_x, cHF_y, cTP_x and cTP_y)

2.4. Statistical analysis

The difference between the extracted indices and the indices obtained from gold-standard PRV trends was measured, and the results obtained from applying the different filters within each of the combination of noises were compared using factorial analyses, in order to evaluate which combination of cutoff frequencies, filter type and filter topology gave the most accurate results for each type of signal. Since these differences did not follow a normal distribution as confirmed by Lilliefors tests, Box–Cox transformations were applied in each case, and the factorial analyses results were derived after these transformations. A 95% significance value was used for all the analyses.

3. Results

3.1. Signal simulation

Figs. 5 and 6 depict excellent and acceptable signals simulated with the different noise combinations, respectively. As expected, as the number of noise components increases, the complexity of the signal is higher and, most likely, it would be more difficult to obtain a good quality filtered PPG and to extract PRV information from these signals.

3.2. Factorial analyses

Factorial analyses with Box–Cox transform were performed for each group of signals with a particular combination of noises, to evaluate the impact of the type of filter and cutoff frequencies on PRV analysis when contaminated PPG signals with each noise were analysed. It was found that the three factors, i.e., the type of filter and its cutoff

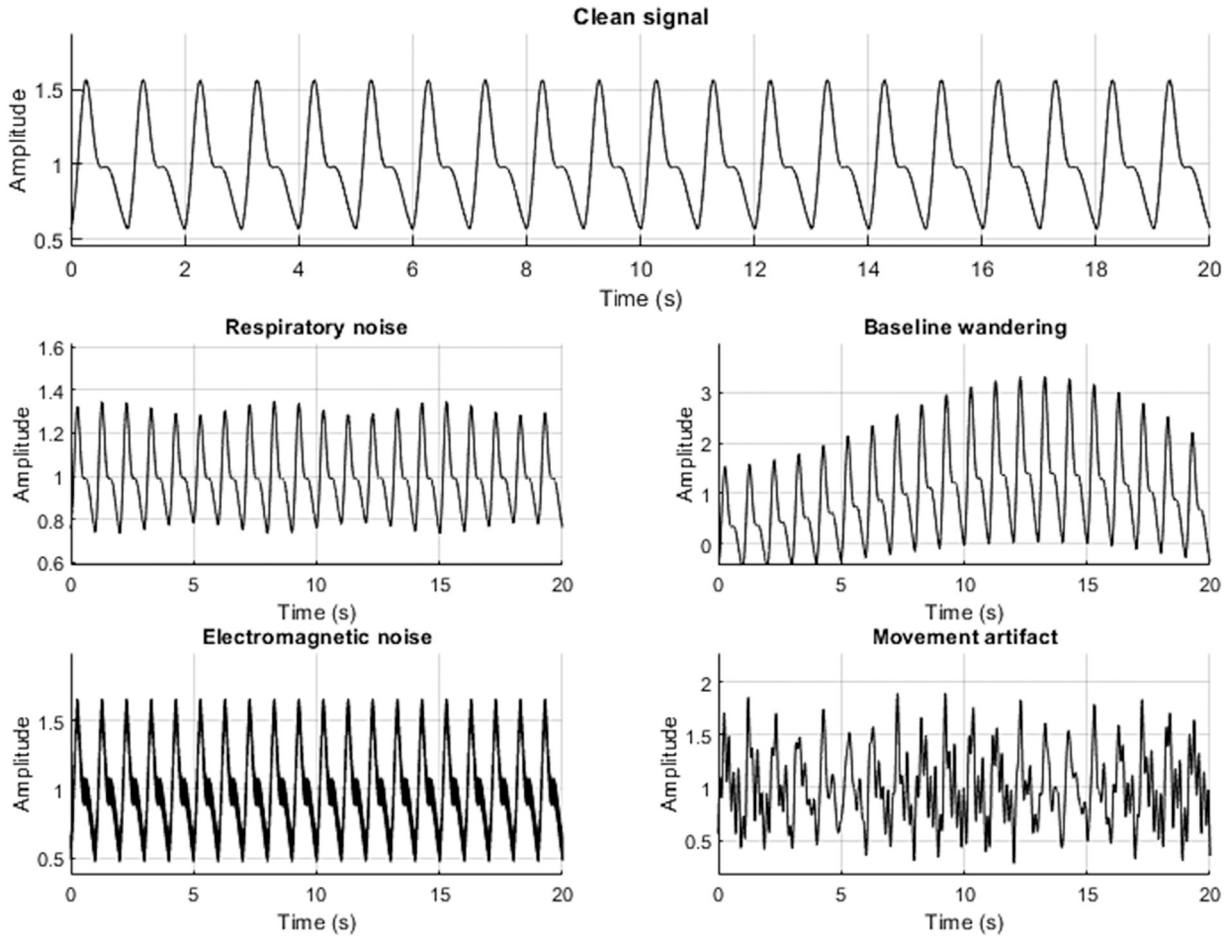

Fig. 4. Behaviour of the different types of noise on the simulated PPG signals.

frequencies, have a significant effect in most PRV indices, as well as their interactions, when excellent and acceptable quality PPG signals were used, and these were contaminated with different kind of noises. The x-coordinates of centroid-related indices tended to be less affected by the interaction of factors than the other indices.

The combinations of factors that gave the lowest difference to gold standard indices were determined for each combination of noises. Figs. 7 and 8 show the average and standard deviation of the absolute differences between PRV indices obtained from measured and gold-standard PRV trends for excellent and acceptable quality PPG signals, respectively. The pNN50 index is not shown given the extremely large differences shown in the measurement of this index, probably due to the presence of outliers in the detection of IBIs from contaminated PPG signals. Therefore, care should be taken when this particular index is measured from PRV extracted from noisy PPG signals regardless of the filtering strategy used.

Besides pNN50 and considering the other PRV indices obtained from noise contaminated, excellent quality PPG signals, frequency-domain indices showed a relatively stable difference to gold standard, regardless of the type of noise, with VLF showing the largest differences to gold standard. Time-domain and Poincaré plot indices did show changes in the differences due to the noise present in the signal. Interestingly, the more complex the noise, the lower differences were obtained after filtering the PPG signal with optimal parameters. For these indices, AVNN was the most affected one. A similar behaviour can be observed when PRV is obtained from noise-contaminated acceptable quality PPG signals.

The most common parameters that gave the lowest differences for each of the types of noise are shown in Tables 3 and 4, for excellent and acceptable quality PPG signals respectively. It was observed that the extraction of PRV from excellent and acceptable quality PPG signals contaminated with different types of noise tends to be more reliable if the PPG signals are filtered using elliptic IIR filters, or equiripple or Parks–McClellan FIR filters. There were differences in these results due to the different quality of signals, but these three types of filters showed the lowest differences to gold standard indices. Again, it should be remarked that pNN50 showed an unreliable behaviour, and care should be taken when measuring this index from PRV extracted from noise-contaminated PPG signals.

For excellent quality PPG signals and most of the types of noises studied in this experiment, lower low cutoff frequencies gave better results. In the case of high cutoff frequencies, most results showed better performance when 20 Hz was used. Only when movement artifact and respiratory noise, or when movement artifact, respiratory noise and baseline wandering where present in the signal, the high cutoff frequency with better performance was found to be 8 Hz. This could be a result of the frequency content of the movement artifact.

When acceptable quality signals were analysed, the lower low cutoff frequency used, the better results were obtained, with most filters acting as low pass filters. For high cutoff frequencies, a similar pattern was observed as in excellent quality PPG signals.

4. Discussion

PPG-based PRV has been proposed as an alternative to evaluate cardiovascular autonomic activity, instead of HRV acquired from ECG signals. However, the relationship between these two variables is not entirely understood, and there is evidence of both physiological and

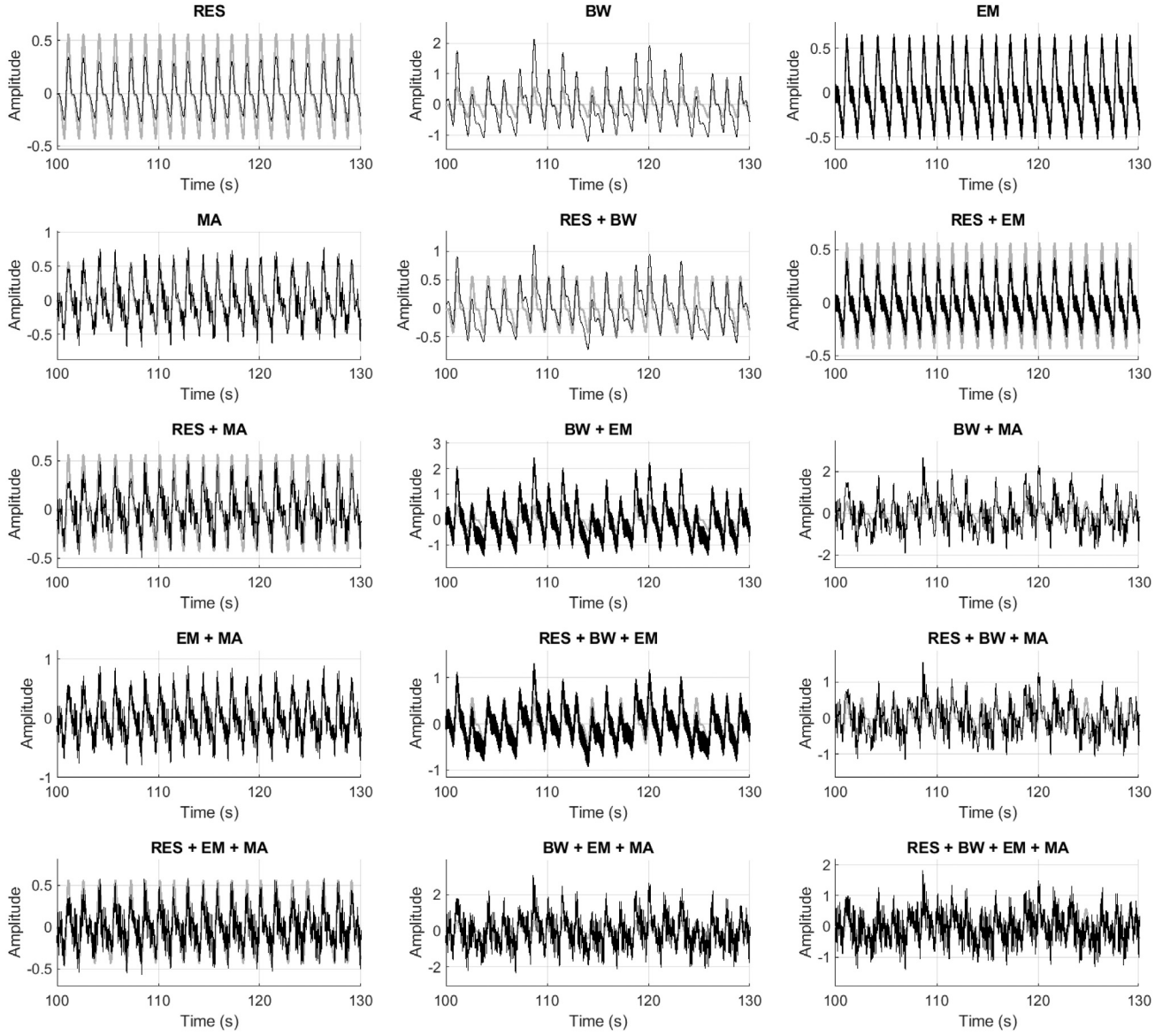

Fig. 5. Example of noise-corrupted, excellent quality photoplethysmographic signals simulated for experiment 6. RES: Respiratory noise; BW: Baseline wandering; EM: Electromagnetic noise; MA: Movement artifact.

technical aspects that may affect PRV differently to HRV [1,17]. Moreover, although guidelines have been proposed for the extraction and analysis of HRV information from ECG signals [2], there is not a standard procedure for the analysis of PRV information from pulse wave signals, specifically from PPGs. In this study, the aim was to evaluate how noise and filtering strategies affected PRV information extracted from simulated signals.

4.1. Signals simulation

Although it is not possible to completely mimic physiological changes in a simulation model, using these approaches for the generation of synthetic PPG signals opens the door for the development and assessment of novel algorithms and techniques that aid in a more efficient and reliable analysis of the PPG signal [10,11]. This is due to the capability of simulating a large number of signals with varying features, such as sampling rate, mean heart rate or the quality of the signal. Moreover, it allows for the analysis of signals in a controlled environment, in which no physiological or environmental factors can affect the information obtained from the PPG. For this particular study, it was possible to generate a large database with PPG signals contaminated with specific types of noise, which allows for a better understanding of how each of these noises may be neutralised for a reliable PRV analysis from PPG signals.

The capability of simulating several types of noise with different parameters is one of the main contributions of the proposed framework and, considering the susceptibility of PPG signals to noise, having a simulation framework that includes different types and magnitude of noises could help in the development and testing of robust algorithms for PPG signal processing, not only for PRV analysis. Further types of noise could be modelled and included in the framework, but the currently used types of noise were considered due to its effect on PPG signals.

4.2. Noise management

The application of filters in the PPG signal is essential to improve its signal-to-noise ratio (SNR), which tends to be low due to the multiple artifacts that may affect it [3,18,19]. However, these filters may also

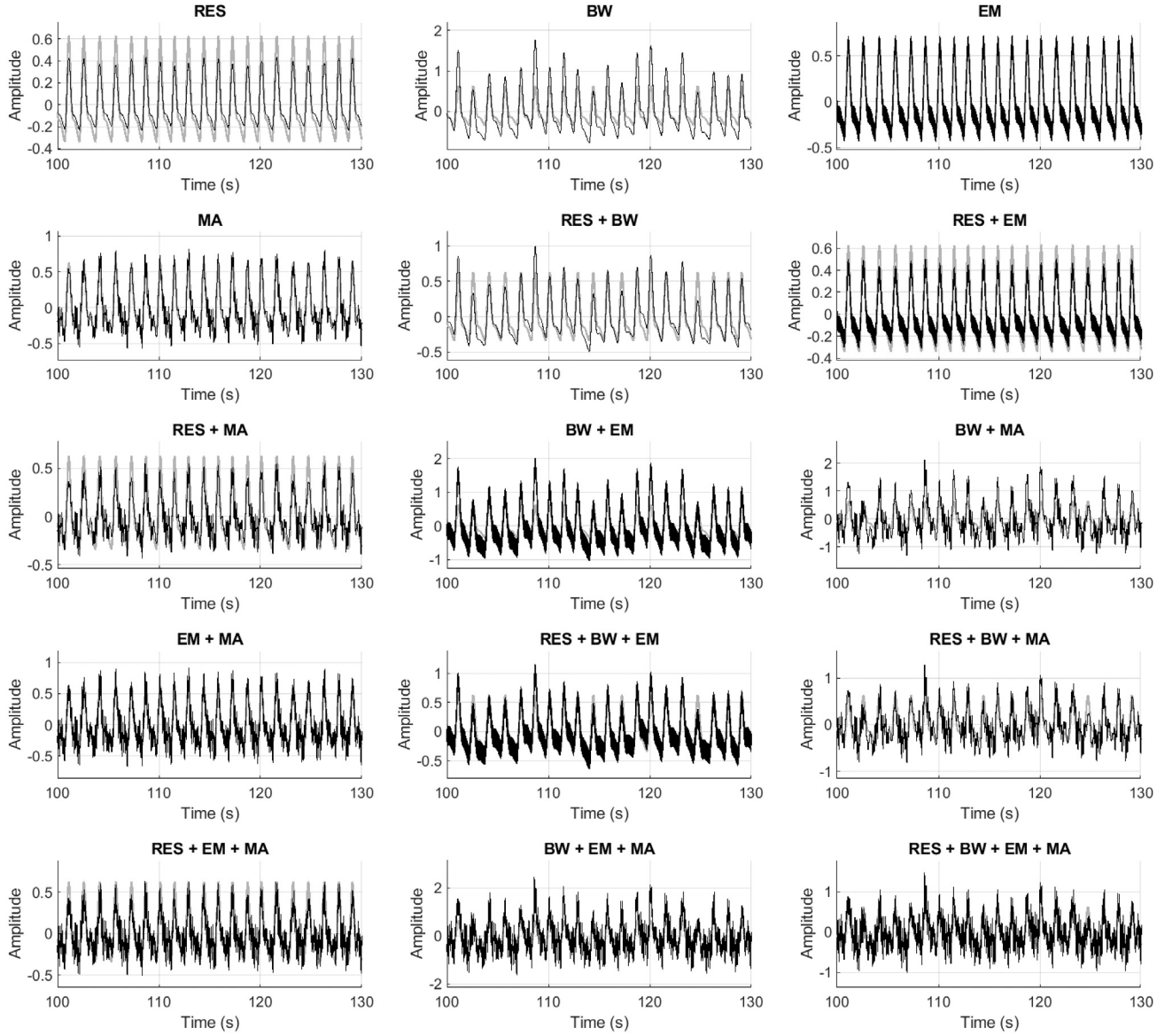

Fig. 6. Example of noise-corrupted, acceptable quality photoplethysmographic signals simulated for experiment 6. RES: Respiratory noise; BW: Baseline wandering; EM: Electromagnetic noise; MA: Movement artifact.

generate changes in the PPG waveform that could affect the identification of fiducial points from the signal and, hence, affect the reliability of PRV information. Moreover, the filters could induce time-shifts in the detection of fiducial points that could determine the reliability of the PRV information extracted from the signal [20].

In this study, each combination of noises was treated independently, since in most cases it is possible to identify the noise present in real PPG signals, and the filtering strategies to each of types of noise can significantly vary. In line with this, it was observed that, regardless of the combination of noise present in the PPG signal, the filter applied and its cutoff frequencies had a significant effect on most PRV indices. Perhaps the most robust index from PRV was the x-coordinates of centroid-related, indicating the robustness of these indices above those related with the magnitude of frequency bands.

It is important to discuss the particular behaviour of pNN50. This index showed important differences against gold-standard indices, regardless of the noise and the filters applied. Hence, care should be taken when this index is analysed from PRV trends extracted from noise-contaminated signals, given it is largely affected by outliers in the trends. For the other indices, a similar behaviour between excellent and acceptable quality, noise-contaminated PPG signals was observed. Interestingly, for time-domain and Poincaré plot indices the differences to gold standard tended to become smaller as the noise combination became more complex. For frequency-domain indices, the differences tended to remain stable, especially for relative and x-coordinate related indices. Time-domain and Poincaré plot indices showed larger differences to gold standard than frequency-domain indices, from which VLF was the index that showed larger differences. This could be explained by the fact that PRV was extracted from short 5-min PPG signals, contaminated with noise, which could have an important effect on the frequency spectra and the near DC components of the signal. Nonetheless, it was observed that, applying the best performance filtering strategies, the differences to gold standard can be considered acceptable.

In general, it was observed that PRV indices tend to show better reliability when PPG signals are filtered using elliptic IIR filters or equiripple or Parks–McClellan FIR filters. In terms of cutoff frequencies, lower low cutoff frequencies tended to give better results, except for those excellent quality PPG signals contaminated with a combination of baseline wandering, movement artifact and respiratory noise,

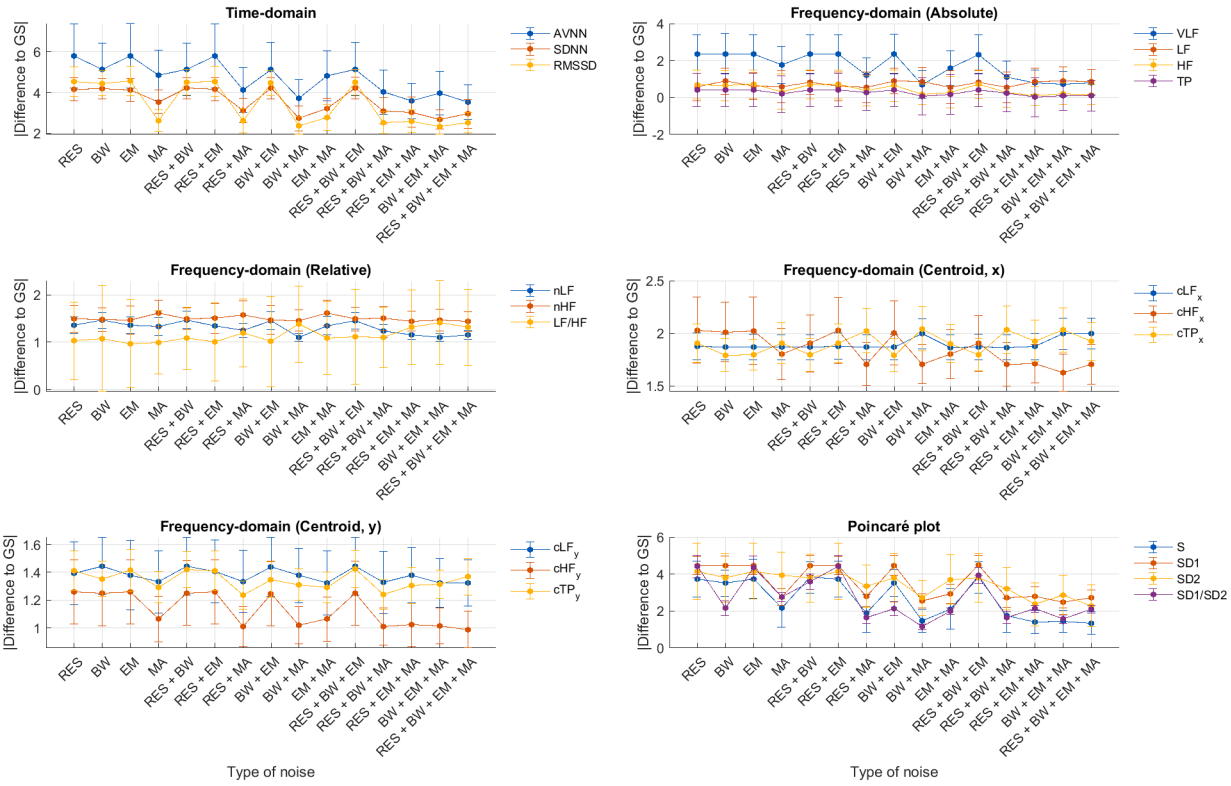

Fig. 7. Mean and standard deviation of absolute differences between pulse rate variability (PRV) indices extracted from excellent quality photoplethysmographic (PPG) signals contaminated with different noises and filtered using the best combination of factors obtained, against indices obtained from gold-standard PRV trends. RES: Respiratory noise. BW: Baseline wandering. EM: Electromagnetic noise. MA: Movement artifact.

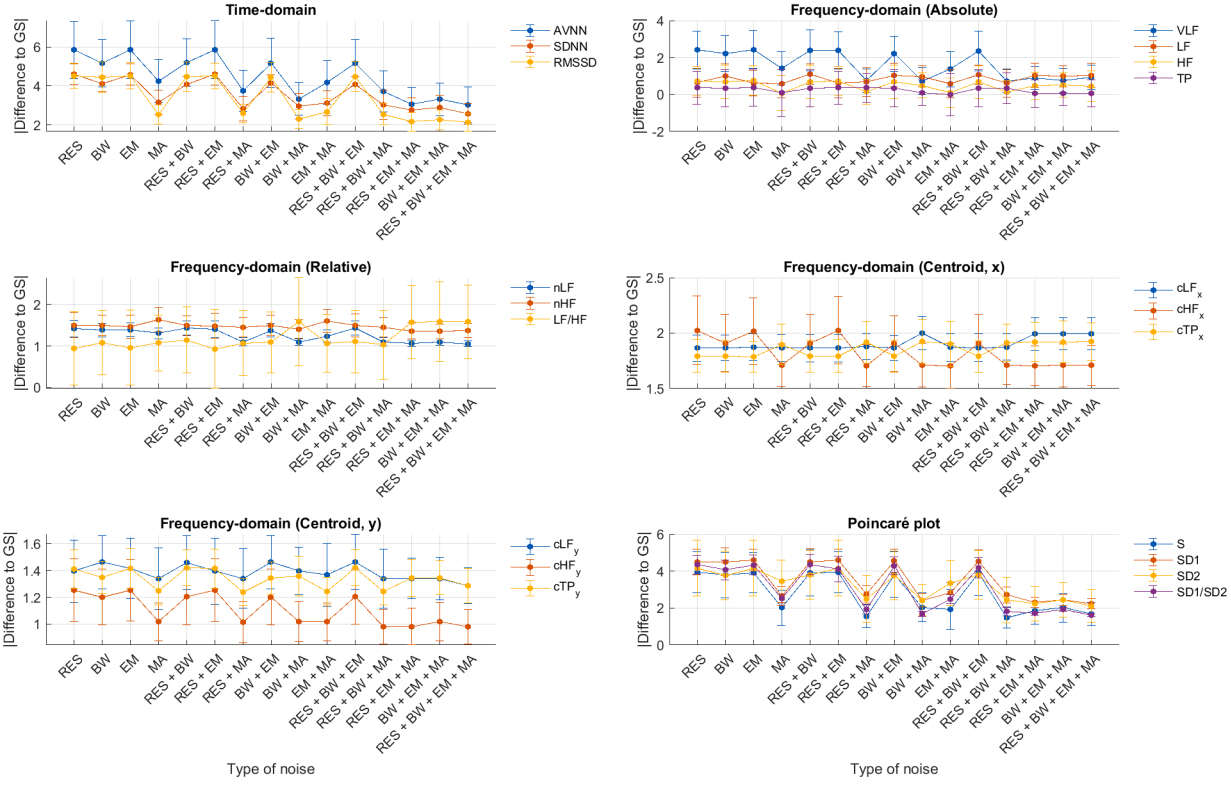

Fig. 8. Mean and standard deviation of absolute differences between pulse rate variability (PRV) indices extracted from acceptable quality photoplethysmographic (PPG) signals contaminated with different noises and filtered using the best combination of factors obtained, against indices obtained from gold-standard PRV trends. RES: Respiratory noise. BW: Baseline wandering. EM: Electromagnetic noise. MA: Movement artifact.

Table 3
Best combination of factors for filtering excellent quality photoplethysmographic signals with different types of noise. FIR: Finite impulse response filters. IIR: Infinite impulse response filters. RES: Respiratory noise. BW: Baseline wandering. EM: Electromagnetic noise. MA: Movement artifact. fc_{low}: Low cutoff frequency. fc_{high}: High cutoff frequency.

Noise	Type of filter	fc_{low} (Hz)	fc_{high} (Hz)
RES	IIR Elliptic	0	20
BW	IIR Elliptic	0	12
EM	IIR Elliptic	0	20
MA	IIR Elliptic	0.2	20
RES + BW	IIR Elliptic	0	20
RES + EM	IIR Elliptic	0.2	20
RES + MA	FIR Equiripple	1	8
BW + EM	IIR Elliptic	0	20
BW + MA	FIR Parks–McClellan	2	12
EM + MA	IIR Elliptic	0.1	20
RES + BW + EM	IIR Elliptic	0.1	20
RES + BW + MA	FIR Equiripple	1	8
RES + EM + MA	FIR Equiripple	0.1	12
BW + EM + MA	FIR Equiripple	0.1	12
RES + BW + EM + MA	FIR Equiripple	0.1	12

Table 4
Best combination of factors for filtering acceptable quality photoplethysmographic signals with different types of noise. FIR: Finite impulse response filters. IIR: Infinite impulse response filters. RES: Respiratory noise. BW: Baseline wandering. EM: Electromagnetic noise. MA: Movement artifact. fc_{low}: Low cutoff frequency. fc_{high}: High cutoff frequency.

Noise	Type of filter	fc_{low} (Hz)	fc_{high} (Hz)
RES	IIR Elliptic	0	20
BW	FIR Parks–McClellan	0	20
EM	IIR Elliptic	0	20
MA	IIR Elliptic	0.1	20
RES + BW	IIR Elliptic	0	12
RES + EM	IIR Elliptic	0	20
RES + MA	FIR Parks–McClellan	0	10
BW + EM	FIR Parks–McClellan	0	20
BW + MA	FIR Parks–McClellan	0	12
EM + MA	FIR Parks–McClellan	0.1	20
RES + BW + EM	IIR Elliptic	0	20
RES + BW + MA	FIR Parks–McClellan	0	10
RES + EM + MA	FIR Equiripple	0	8
BW + EM + MA	FIR Parks–McClellan	0.5	15
RES + BW + EM + MA	FIR Equiripple	0.5	8

which needed higher low cutoff frequencies, most likely due to the frequency content of the respiratory and baseline wandering noises. For higher cutoff frequencies, both with excellent and acceptable quality PPG signals, the most common high cutoff frequency was 20 Hz, which was the maximum considered cutoff frequency. This could be an indication of the more important role played by the lower cutoff frequency of the filter to remove the types of noises included in this study. Moreover, higher cutoff frequencies affect less the morphology of the anacrotic phase of the pulse, probably allowing a more precise detection of the fiducial point used in this study. These results are in line with the results obtained in a similar study performed with data obtained from healthy, resting subjects and by comparing PRV to HRV information [21].

Other studies have aimed to understand the effects of digital filtering on PRV. Akar et al. [22] concluded that using a Butterworth filter and a nonlinear weighted Myriad filter did not have a significant difference on PRV analysis. Kim and Ahn [23] evaluated the effects of Butterworth and elliptic filters for the assessment of PRV from PPG signals, and concluded that there were no significant differences between HRV and PRV time series, although small differences were observed in some extracted indices. The results found in this study indicate differences in the type of filter and its parameters used given the different types of noise involved in the signal, which is a factor that has not been taken into account in previous studies and could explain, to some extent, the differences in results. Nonetheless, the present study involves a large data set and multiple different factors that were not included in these previous studies. Further studies should aim to validate the obtained results in real data with different but controlled types of noise.

4.3. Limitations of the study

This study has some limitations. Firstly, simulated PPG signals with simulated PRV information were used in this study. This was done with two main purposes. It is simpler to obtain a larger number of samples using simulated data, which gives statistical validity to the experiment. The sample size for each of the experiments in this study was estimated to be the optimal value in order to observe differences of 2% in the measurement of the indices, compared to the gold standard. Also, by simulating PRV information it was possible to obtain a gold standard that was not HRV information obtained from the ECG. As mentioned, physiological aspects may explain part of the differences between HRV and PRV, hence comparing them in order to establish methodologies and strategies for obtaining PRV information is not ideal. Regardless of the benefits, using simulated PPG signals may not represent the entire variation of the PPG morphology, and the results from these experiments need to be validated using real PPG data. The simulation of PRV information may also affect the results obtained. However, PRV was simulated using physiologically feasible values, which may introduce larger variability of the PRV but also simulate PRV information that could be obtained from most of the healthy population. Future studies could optimise the PRV model to have a better reflection of real PRV information.

The simulation of noise and the models used can also be considered a limitation. Future studies should aim to better model these noises and include other types of noise that might be involved in PPG signals, such as those generated from the acquisition systems or other physiological phenomena. Finally, the agreement between indices was not assessed. Future studies should investigate not only the significance of the difference but also determine how the indices agree using techniques such as Bland–Altman analysis.

CRediT authorship contribution statement

Elisa Mejía-Mejía: Conceptualization, Methodology, Software, Formal analysis, Investigation, Data curation, Writing – original draft, Visualization. **Panicos A. Kyriacou:** Conceptualization, Resources, Writing – review & editing, Supervision, Project administration.

Declaration of competing interest

The authors declare that they have no known competing financial interests or personal relationships that could have appeared to influence the work reported in this paper.

Data availability

Data will be made available on request.

References

[1] E. Mejía-Mejía, J. May, R. Torres, P. Kyriacou, Pulse rate variability in cardiovascular health: a review on its applications and relationship with heart rate variability, Physiol. Meas. 41 (2020) 07TR01, http://dx.doi.org/10.1088/1361-6579/ab998c.

[2] Task Force of the European Society of Cardiology and The North American Society of Pacing and Electrophysiology, Heart rate variability: Standards of measurement, physiological interpretation, and clinical use, Circulation 93 (1996) 1043–1065, http://dx.doi.org/10.1161/01.CIR.93.5.1043.

[3] P. Kyriacou, Introduction to photoplethysmography, in: P. Kyriacou, J. Allen (Eds.), Photoplethysmography: Technology, Signal Analysis, and Applications, Elsevier, London, UK, 2021, pp. 1–15.

[4] E. Mejía-Mejía, K. Budidha, T. Abay, J. May, P. Kyriacou, Heart rate variability (HRV) and pulse rate variability (PRV) for the assessment of autonomic responses, Front. Physiol. 11 (2020) 779, http://dx.doi.org/10.3389/fphys.2020.00779.

[5] E. Mejía-Mejía, J. May, M. Elgendi, P. Kyriacou, Differential effects of the blood pressure state on pulse rate variability and heart rate variability in critically ill patients, Npj Digit. Med. 4 (2021) 82, http://dx.doi.org/10.1038/s41746-021-00447-y.

[6] I. Constant, D. Laude, I. Murat, J.-L. Elghozi, Pulse rate variability is not a surrogate for heart rate variability, Clin. Sci. 97 (1999) 391–397.

[7] K. Charlot, J. Cornolo, J.V. Brugniaux, J. Richalet, A. Pichon, Interchangeability between heart rate and photoplethysmography variabilities during sympathetic stimulations, Physiol. Meas. 30 (2009) 1357–1369, http://dx.doi.org/10.1088/0967-3334/30/12/005.

[8] E. Gil, M. Orini, R. Bailón, J.M. Vergara, L. Mainardi, P. Laguna, Photoplethysmography pulse rate variability as a surrogate measurement of heart rate variability during non-stationary conditions, Physiol. Meas. 31 (9) (2010) 1271–1290, http://dx.doi.org/10.1088/0967-3334/31/9/015.

[9] E. Mejía-Mejía, J. May, P. Kyriacou, Effects of using different algorithms and fiducial points for the detection of interbeat intervals, and different sampling rates on the assessment of pulse rate variability from photoplethysmography, Comput. Methods Prog. Biol. 218 (2022) 106724, http://dx.doi.org/10.1016/j.cmpb.2022.106724.

[10] Q. Tang, Z. Chen, R. Ward, M. Elgendi, Synthetic photoplethysmogram generation using two Gaussian functions, Sci. Rep. 10 (2020) 13883, http://dx.doi.org/10.1038/s41598-020-69076-x.

[11] Q. Tang, Z. Chen, J. Allen, A. Alian, C. Menon, R. Ward, M. Elgendi, PPGSynth: An innovative toolbox for synthesizing regular and irregular photoplethysmography waveforms, Front. Med. (Lausanne) 7 (2020) 597774, http://dx.doi.org/10.3389/fmed.2020.597774.

[12] B. Moody, G. Moody, M. Villarroel, G. Clifford, I. Silva, MIMIC-III waveform database (version 1.0), physionet, 2020, Online, url: https://doi.org/10.13026/c2607m.

[13] A. Johnson, T. Pollard, L. Shen, L. Lehman, M. Feng, M. Ghassemi, B. Moody, P. Szolovits, L. Celi, R. Mark, MIMIC-III, a freely accessible critical care database, Sci. Data 3 (2016) 160035, http://dx.doi.org/10.1038/sdata.2016.35.

[14] A. Goldberger, L. Amaral, L. Glass, J. Hausdorff, P. Ivanov, R. Mark, J. Mietus, G. Moody, C. Peng, H. Stanley, PhysioBank, PhysioToolkit, and PhysioNet: Components of a new research resource for complex physiologic signals, Circulation 101 (2000) e215–e220, http://dx.doi.org/10.1161/01.cir.101.23.e215.

[15] S. Béres, L. Hejjel, The minimal sampling frequency of the photoplethysmogram for accurate pulse rate variability parameters in healthy volunteers, Biomed. Signal Process. Control 68 (2021) 102589, http://dx.doi.org/10.1016/j.bspc.2021.102589.

[16] M. Elgendi, I. Norton, M. Brearley, D. Abbott, D. Schuurmans, Systolic peak detection in acceleration photoplethysmograms measured from emergency responders in tropical conditions, PLoS One 8 (10) (2013) e76585, http://dx.doi.org/10.1371/journal.pone.0076585.

[17] A. Schäfer, J. Vagedes, How accurate is pulse rate variability as an estimate of heart rate variability? A review on studies comparing photoplethysmographic technology with an electrocardiogram, Int. J. Cardiol. 166 (2013) 15–29, http://dx.doi.org/10.1016/j.ijcard.2012.03.119.

[18] J. Allen, Photoplethysmography and its application in clinical physiological measurement, Physiol. Meas. 28 (2007) R1–R39, http://dx.doi.org/10.1088/0967-3334/28/3/R01.

[19] E. Mejía-Mejía, J. Allen, K. Budidha, C. El-Hajj, P. Kyriacou, P. Charlton, Photoplethysmography signal processing and synthesis, in: P. Kyriacou, J. Allen (Eds.), Photoplethysmography: Technology, Signal Analysis, and Applications, Elsevier, London, UK, 2021, pp. 69–145.

[20] H. Liu, J. Allen, S. Ghufran Khalid, F. Fei Chen, D. Zheng, Filtering-induced time shifts in photoplethysmography pulse features measured at different body sites: the importance of filter definition and standardization, Physiol. Meas. 42 (2021) 074001, http://dx.doi.org/10.1088/1361-6579/ac0a34.

[21] E. Mejía-Mejía, J. May, P. Kyriacou, Effect of filtering of photoplethysmography signals in pulse rate variability analysis, in: Annu Int Conf IEEE Eng Med Biol Soc, 2021, pp. 5500–5503, http://dx.doi.org/10.1109/EMBC46164.2021.9629521.

[22] S. Akar, S. Kara, F. Latifolu, V. Bilgiç, Spectral analysis of photoplethysmographic signals: The importance of preprocessing, Biomed. Signal Process. Control 8 (2013) 16–22, http://dx.doi.org/10.1016/j.bspc.2012.04.002.

[23] J. Kim, J. Ahn, Digital IIR filters for heart rate variability; A comparison between butterworth and elliptic filters, Int. J. Sci. Technol. Res. 8 (2019) 3509–3513.